

# Enhanced-Performance Wireless Conformal "Smart Skins" Utilizing Inkjet-Printed Carbon-Nanostructures

Taoran Le<sup>1</sup>, Ziyin Lin<sup>2</sup>, C. P. Wong<sup>2</sup>, and M. M. Tentzeris<sup>1</sup>

<sup>1</sup>School of Electrical and Computer Engineering, <sup>2</sup>School of Materials Science and Engineering  
Georgia Institute of Technology  
Atlanta, GA 30332  
taoran.le@ece.gatech.edu

## Abstract

This paper introduces for the first time the integration of a UHF radio frequency identification (RFID) antenna with reduced graphene oxide (rGO), developed using direct-write techniques and utilizing an RFID chip for chemical gas detection. The module is realized by inkjet printing on a low-cost paper-based substrate, and the RFID tag is designed for the North America UHF RFID band. The electrical impedance of the rGO thin film changes in the presence of very small quantities of certain toxic gases, resulting in a variation of the backscattered power level which is easily detected by the RFID reader to realize reliable wireless toxic gas sensing. The inkjet printed RFID tag demonstrated a change in backscattered power of 9.18% upon exposure of 40 ppm NO<sub>2</sub> for 5 minutes.

**Index Terms** — *Gas sensor, graphene, inkjet printing, UHF RFID, wireless, T-match.*

## I. Introduction

The strict demands to both business and process in today's industry require robust, accurate sensors developed using low cost, reliable fabrication methods. In addition, uses such as environmental cognition require a robust sensor with extremely low power consumption. Therefore, methods for development of accurate, low power sensors using proven, low cost fabrication systems and off the shelf (OTC) components are extremely desirable. This paper provides detail and design of a sensor developed using conventional inkjet printing methods and OTC RFID components to create an accurate, robust, low power wireless gas detection system.

Carbon materials, such as carbon nanotube (CNT) and graphene, have been investigated previously as candidates for the early and accurate detection of various chemicals [1-3]. These materials alter their properties in the presence of a given substance due to their ability to absorb the chemicals on their surface [4-5]. Chemical absorption produces changes in material properties such as real and imaginary impedance, DC resistance, and effective dielectric constant [1]. These changes can be exploited to determine the presence of various chemical compounds by translating the material effects into measurable electrical quantities such as changes in voltage, current, resonant frequency, and backscattered power amplitude. Excellent electrical conductivity and the ability to be functionalized for a wide range of chemicals make these novel materials ideal candidates for the development of a broad spectrum of portable and wearable sensors. Moreover, the ability to deposit these materials via inkjet printing of

aqueous solutions on low cost, flexible, environmentally friendly substrates opens the possibility of mass producing such devices and taking advantage of economies of scale.

In our previous research efforts, we have demonstrated excellent gas detection sensitivity for nitrogen-based gases [1,6]. At 10ppm NO<sub>2</sub> we achieved 21% sensitivity, and at 4ppm NH<sub>3</sub> a 9% sensitivity was obtained at 864 MHz using functionalized multi walled CNT (MWCNT) dissolved in water and inkjet printed on paper substrate. The incorporation of the previous graphene-based sensing thin films with micro-strip lines served as proof of concept [2, 6]. Of course these transmission lines can be thought of as parts of a wide range of antenna and microwave structures. Under this analog transmission approach, the wireless remote sensing mechanism is actually the detection of shifts in resonant frequency and / or magnitude of the backscattered power as a direct result of the change in impedance of the graphene stripes and, thus, also of the whole structure. Calibration may be needed in order to map particular amounts of shift in the resonant frequency or change in backscattered power levels to the concentration of toxic gases under test.

This paper will establish for the first time the principles of wireless gas sensor design utilizing rGO based thin films integrated into RFID platforms, and featuring the first ever inkjet-printing of aqueous graphene oxide solution on environmentally friendly paper. Use of water based carbon inks and paper substrates can set the standard for the development of a class of low cost, environmentally friendly rGO based sensors utilizing RFID principles.

## II. Passive UHF RFID Tag Design

### A. General Design Consideration for rGO based Inkjet-Printed Gas Sensor Tags

In the previous work on SWCNT based wireless gas sensors [7], a passive RFID system was utilized. This work uses a similar methodology. The RFID reader sends an interrogating RF signal to the RFID tag, which contains an antenna and an IC chip. The IC responds to the reader by varying its input impedance, thereby modulating the backscattered radiation levels. The modulation scheme often used in RFID applications is amplitude shift keying (ASK). The IC impedance switches between the matched state and the mismatched state, altering levels of backscattered radiation [8]. As illustrated in Fig.1, the rGO thin film is integrated with the printed antenna by direct-write methods, and acts as a tunable part of the antenna with an impedance value determined by the concentration of the target gas. The RFID reader monitors the backscattered power level. Once the

power level changes, it shows that there is a variation of the rGO film impedance, therefore, the wireless sensor detects the existence and the concentration of the target gas.

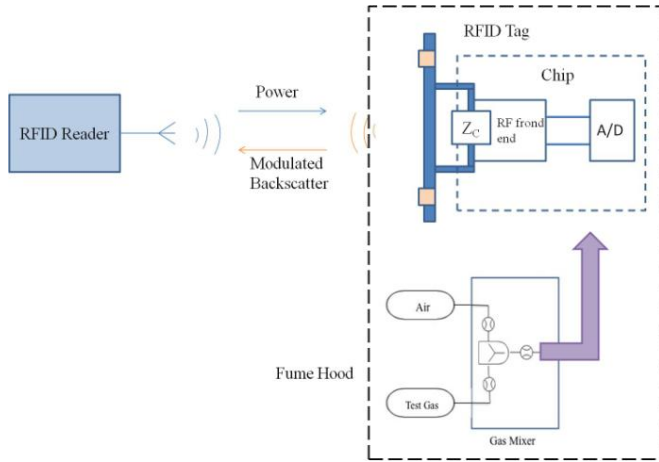


Figure 1. Conceptual diagram of the RFID-enabled wireless gas sensor module.

The power level of the received signal can be calculated using the Friis free-space equation as:

$$P_{tag} = P_t G_t G_r \left( \frac{\lambda}{4\pi d} \right)^2 \quad (1)$$

where  $P_t$  is the power transmitted from the reader antenna,  $G_r$  and  $G_t$  are the gains of the reader antenna and the tag antenna respectively, and  $d$  is the distance between the reader and the tag.

### B. Tag Antenna Design Parameters

The design goals for the tag antenna were to achieve an omnidirectional read pattern and maximum read range. Two types of known planar tag antennas which can provide an omnidirectional pattern are a slot antennas and dipole antennas. However, a slot type tag antenna usually requires significantly more metallization and a larger footprint than a dipole. Since a goal of the project was to provide a low cost system, a dipole design was chosen for the tag antenna design.

The maximum read range of a passive UHF RFID tag depends on the gain and quality of impedance matching between the tag antenna and IC [9]. The read range can be optimized by selecting an IC with low-power consumption, maximizing the antenna gain, and arranging a complex-conjugate impedance matching between the IC and tag antenna for maximal power transfer [10]. Two IC chips (SOT 1040AB2 and Higgs-4 SOT) were chosen for design in the North America UHF RFID band. The parameters are listed in the Table I. The power transfer between the antenna and IC is described by a power transmission coefficient (PTC) as:

$$\tau = P_C/P_A \quad (2)$$

where  $P_C$  is the power absorbed by the chip from the antenna, and  $P_A$  is the maximum available power from the antenna.

The maximum power can be transferred when  $Z_C$  is the conjugate value of  $Z_A$  [11].

TABLE I.  
IC Chip Parameters at 915MHz

Symbol	Quantity	Value [ $\Omega$ ]
$Z_{C1}$	SOT 1040Ab2 IC impedance	13.3- j122
$Z_{A1}$	Tag 1 antenna design impedance	13.1+ j122
$Z_{C2}$	Higgs-4 SOT IC impedance	18.5- j181.3
$Z_{A2}$	Tag 2 antenna design impedance	18.5+ j 181.3

The T-match is an effective way modify the input impedance of a dipole by introducing a centered short-circuit stub, as shown in Fig.2 [12].

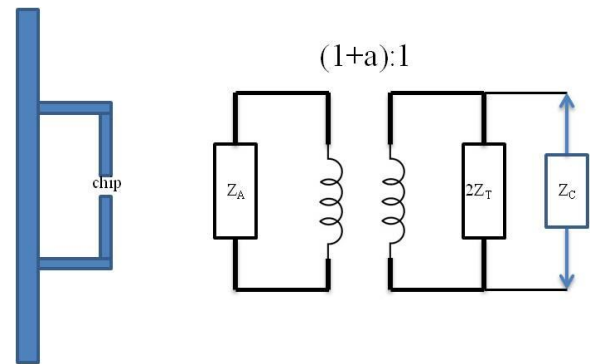


Figure 2. T-match configuration for dipoles and equivalent circuit.

The terminal impedance is given by [13],

$$Z_{in} = \frac{2Z_T(1 + \alpha)^2 Z_A}{2Z_T + (1 + \alpha)^2 Z_A} \quad (3)$$

where ( $Z_T = jZ_0 \tan \alpha/2$ ) is the input impedance of the short-circuit stub by the T-match circuit and the middle part of the dipole. Preliminary results demonstrate that the surface area of the inkjet-printed graphene rather than the number of its inkjet-printed layers determine the sensitivity to the presence of small concentrations of poisonous gases [14]. Therefore, as long as the surface area of the rGO exposed to the air remains constant, the gas sensitivity remains the same. Two antenna tags with two different surface area rGO film patterns were designed in Computer Simulation Technology (CST) STUDIO SUITE® 2013 for validating and optimizing the gas sensor sensitivity. The parameters used to model the inkjet-printed conductor are listed in the Table II. The Kodak photopaper substrate parameters are the same as used in the previous work [15]. The Cabot silver ink was also used, as in [16].

TABLE II.  
Design Specifications

Symbol	Quantity	Value
$f_0$	Operating frequency	915 MHz
$\epsilon_r$	Dielectric constant	2.9
H	Paper thickness	230 $\mu\text{m}$
Tan $\delta$	Loss tangent of paper	0.05
T	Carbot silver ink thickness	1.6 $\mu\text{m}$
$\sigma$	Cabot silver ink conductivity	$5e^6$ S/m

The tag antenna design for SOT 1040AB2 IC chip is shown in Fig.3. The antenna tag design for Higgs-4 SOT IC chip is in Fig.4.

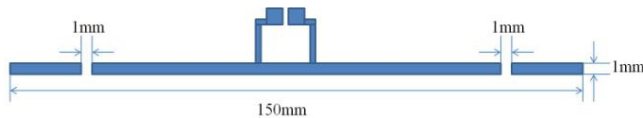


Figure 3. Antenna design for SOT 1040AB2.

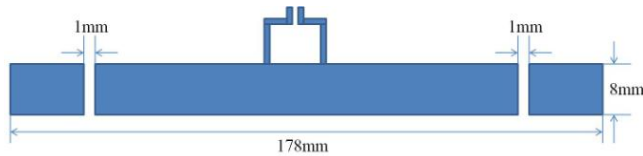


Figure 4. Antenna design for Higgs-4 SOT.

### III. Inkjet Printing of Gas Sensor Prototype

The core of the wireless gas sensor is a prototype board made from graphene deposited onto a Kodak photo paper. Graphene was chosen for several reasons. First, it exhibits remarkable electronic and mechanical properties [3, 5], and graphene oxide materials can be easily dispersed in water. In our previous work on CNT based wireless gas sensors, the short lifetime and poor dispersion of the CNT ink limited the obtainable material performance [1, 7].

Cabot's CCI-300 conductive nanoparticle silver ink was used to create the traces connecting the graphene pad to the external circuitry. Microstrip topology was chosen because the microstrip elements can be easily integrated with inkjet printed rGO thin films.

The tag creation process, shown in Fig. 5, includes:

- 1) Deposition of the GO ink on paper substrate
- 2) Curing and reduction of the GO thin film
- 3) Alignment of the GO film and printing of the antenna
- 4) Sintering of the silver ink
- 5) Integration of the target RFID IC chip on the tag

The following sections will provide a more in depth discussion of these steps.

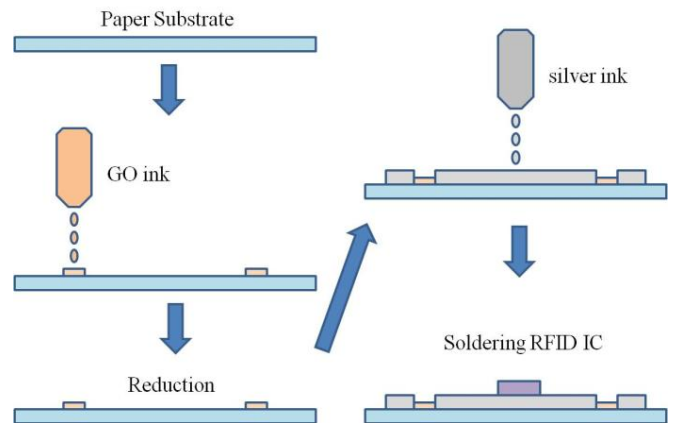


Figure 5. The fabrication process of the gas sensor prototype.

#### A. Creation of Graphene Oxide

The first step in the sensor development process was the creation of stable, long-life, inkjet-printable graphene-based inks. This was accomplished by first converting the graphene into graphene oxide powder. Unlike pristine graphene, which has very poor dispersion in common solvents, graphene oxide (GO) exhibits excellent solubility in water due to the existence of hydrophilic functional groups on the surface [17], rendering it an excellent candidate for development of environmental friendly water-based inks. After deposition, the graphene was restored by the reduction of GO, which reverts the conjugated basal plane and restores the electrical properties of the material. The reduction of GO is considered as one of most promising methods for low-cost, high-yield and scalable preparation of graphene materials [18].

The GO was produced by chemical oxidation of graphite, which introduces oxygen-containing functional groups to exfoliate pristine graphite into individual GO sheets [2, 19]. To prepare the GO ink, dry GO powder was dispersed in a water/glycerol solution and sonicated to form a homogenous dispersion.

#### B. Fabrication via Inkjet Printing

A Dimatix Materials Printer (DMP-2800) Series material deposition system, as shown in Fig. 6, was used to print both the silver and GO inks.

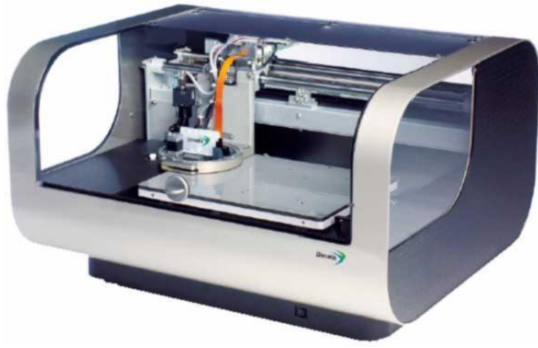


Figure 6. The Dimatix materials printer.

Based on the previous experimentation, we determined that the application of additional 5 layers of silver applied on top of the graphene guarantees better connectivity between the graphene and silver traces and helps to de-embed any additional impedance which would offset the measured change of impedance unevenly among different samples of the similar dimensions [2]. The fabrication process involved deposition 5 layers of GO ink followed by 5 layers of conductive silver onto the paper substrate. First, the 5 layers of GO ink were deposited and cured at 80°C overnight. After the decution of GO thin film, 5 layers silver GO were deposited and cured at 120°C for 30 minutes. To insure optimum contact between the rGO thin film and the silver ink, a 0.5 mm overlap of the two surfaces was chosen.

### C. Reduction of Graphene Oxide

After curing GO ink, chemical oxidation was used to remove some of oxygen-containing groups and restore the conjugated system and the electrical conductivity. Typical methods for GO reduction include thermal reduction,  $N_2H_4$  reduction and  $NaBH_4$  reduction etc. The final structure of chemically reduced graphene is highly dependent on the reduction method, and it is possible to control the final structure by selective removal of specific types of oxygen-containing groups for optimized material properties. Due to the paper substrate thermal tolerances, the  $N_2H_4$  reduction was chosen. The GO thin film was reduced by  $N_2H_4$  vapor at 90 °C overnight.

### D. Final Packaging Steps

The final step in the fabrication was to solder the IC chips to their respective antennas, as shown in Figs. 7 and 8 below



Figure 7. The antenna tag with SOT 1040AB2 .



Figure 8. The antenna tag with Higgs-4 SOT.

### E. Optimization of the Reduced Graphene Oxide Thin Film

Optimization of the RGO thin films was done in order to obtain the proper sensor area to ensure maximum sensitivity. To determine the optimum sensor area, two patterns of different lengths of RGO material were produced as shown in Fig. 3 and Fig. 4. From the previous work in [14], it was expected that the larger surface area of the rGO pattern in Fig. 4 would yield the higher sensitivity.

## IV. Gas Sensor Experimentation

### A. Experiment Setup

The gas test setup is shown in Fig. 9 below. The tags were tested using a KIN-TEK FlexStream gas standards generator to provide a stable gas source with accurate concentrations. The setup was capable of producing reliable mixtures up to 50 ppm of nitrogen dioxide gas diluted in nitrogen gas. A Tagformance Lite RFID reader (Voyantic Inc. 2011) is adopted for interrogation power threshold measurements. At each frequency point, the reader varies the interrogation power until the power is just enough to activate the RFID chip. After the reader sweeps through the entire target frequency range from 800MHz to 1GHz, the interrogation power threshold versus frequency curve can be obtained. When the antenna sensor deforms due to gas, the antenna resonance frequency changes accordingly. Therefore, gas sensing is achieved utilizing the relationship between antenna power threshold and gas concentration.

To begin the test, the reader was first calibrated using a reference tag at a distance of 0.3m away from the reader antenna. Then, the antenna tag was placed at the exact interrogation position as the reference tag. The reader recorded the sweep from 800MHz to 1GHz. Nitrogen was then flowed through the system for 5 minutes to establish a system baseline. Next, the 40 ppm nitrogen dioxide was introduced into the system and the reader swept the entire frequency range again. Finally, the gas source was removed from the device while measurements continued to be taken for another 5 minute interval in order to measure the recovery time of the sensor.

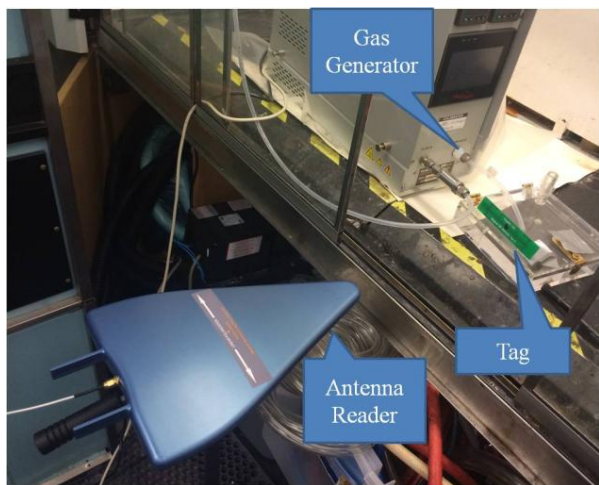


Figure 9. Gas test setup for sensor measurements.

### B. Experimental Results

The results of 40 ppm  $\text{NO}_2$  gas testing are shown in Fig. 10. The inkjet-printed rGO thin films of different dimensions demonstrated similar responses to 40 ppm  $\text{NH}_3$ . Due to the poor connection of the Higgs-4 SOT IC with the antenna, the result was not able to be validated. Fig. 10 shows the power threshold measurement of the antenna tag with SOT 1040AB2 IC. After exposure to the target gas, the mismatching of the impedance between antenna and IC chip caused the backscattered power level to be reduced as compared to the original power level around 915MHz target frequency. The power level of 9.18% difference was observed at the target frequency. After 5 minutes period of pure nitrogen purging, full recovery of the system was observed. We are presently continuing investigations into further improving the recovery time.

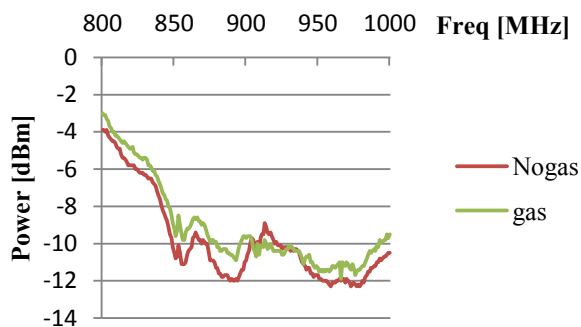


Figure 10. Measured response of RGO thin films with and without  $\text{NO}_2$ .

### VI. Conclusion

We have demonstrated for the first time integration of rGO thin films onto an inkjet printed UHF RFID module on paper to form a wireless gas sensor. We also provide detailed results of our efforts in the development of environmentally friendly, stable, low cost, inkjet-printable GO inks. The design demonstrated the viability of inkjet-printed rGO for the realization of fully integrated “green” wireless RFID-enabled flexible sensors and the ultrasensitive impedance properties of the rGO materials utilized.

The prototype device exceeded our expectations for initial tests, producing a 9.18% change in backscattered power level at 40 ppm concentration of nitrogen dioxide gas. Moreover, the sensor demonstrated fast recovery time in comparison to the current state of technology without the use of heat or UV treatments to assist in the material recovery, providing an advantageous result for sensing in natural environmental conditions.

### V. Future work

Future work includes several areas of improvement on the current design, now that the concept has been proven. The dipole antenna design can be optimized to minimize its size for accommodation of mobile and wearable sensing applications. A meander line design is currently being considered for the generation II prototype. The RFID tag range can also be improved in the next generation, and more directional designs may be considered. Finally, based on the findings here, the sensor sensitivity can be improved by incorporating larger surface area rGO thin films into the design. This is also under consideration in choosing the design parameters of the generation III prototype.

### Acknowledgments

The authors would like to thank NSF-ECS for their support of the research, and the helpful discussion with coworkers John Kimionis, Sangkil Kim and James Cooper.

### References

1. Lakafosis, Vasileios, Xiaohua Yi, Taoran Le, Edward Gebara, Yang Wang, and Manos M. Tentzeris. "Wireless sensing with smart skins." In *Sensors*, 2011 IEEE, pp. 623-626. IEEE, 2011.
2. Le, Taoran, Vasileios Lakafosis, Ziyin Lin, C. P. Wong, and M. M. Tentzeris. "Inkjet-printed graphene-based wireless gas sensor modules." In *Electronic Components and Technology Conference (ECTC)*, 2012 IEEE 62nd, pp. 1003-1008. IEEE, 2012.
3. Geim, Andre K., and Konstantin S. Novoselov. "The rise of graphene." *Nature materials* 6, no. 3 (2007): 183-191.
4. Schedin, F., A. K. Geim, S. V. Morozov, E. W. Hill, P. Blake, M. I. Katsnelson, and K. S. Novoselov. "Detection of individual gas molecules adsorbed on graphene." *Nature materials* 6, no. 9 (2007): 652-655.
5. Li, Dan, and Richard B. Kaner. "Graphene-based materials." *Nat Nanotechnol* 3 (2008): 101.
6. Le, Taoran, Ziyin Lin, C. P. Wong, and M. M. Tentzeris. "Novel enhancement techniques for ultra-high-performance conformal wireless sensors and" smart skins" utilizing inkjet-printed graphene." In *Electronic Components and Technology Conference (ECTC)*, 2013 IEEE 63rd, pp. 1640-1643. IEEE, 2013.
7. Yang, Li, Rongwei Zhang, Daniela Staiculescu, C. P. Wong, and Manos M. Tentzeris. "A novel conformal RFID-enabled module utilizing inkjet-printed antennas and carbon nanotubes for gas-detection applications." *Antennas and Wireless Propagation Letters*, IEEE 8 (2009): 653-656.

8. Nikitin, Pavel V., and K. V. S. Rao. "Performance limitations of passive UHF RFID systems." In *IEEE Antennas and Propagation Society International Symposium*, vol. 1011. 2006.
9. Rao, KV Seshagiri, Pavel V. Nikitin, and Sander F. Lam. "Antenna design for UHF RFID tags: A review and a practical application." *Antennas and Propagation, IEEE Transactions on* 53, no. 12 (2005): 3870-3876.
10. Kurokawa, Kaneyuki. "Power waves and the scattering matrix." *Microwave Theory and Techniques, IEEE Transactions on* 13, no. 2 (1965): 194-202.
11. Rao, KV Seshagiri, Pavel V. Nikitin, and Sander F. Lam. "Impedance matching concepts in RFID transponder design." In *Automatic Identification Advanced Technologies, 2005. Fourth IEEE Workshop on*, pp. 39-42. IEEE, 2005.
12. Balanis, Constantine A. *Antenna theory: analysis and design*. John Wiley & Sons, 2012.
13. Marrocco, Gaetano. "The art of UHF RFID antenna design: impedance-matching and size-reduction techniques." *Antennas and Propagation Magazine, IEEE* 50, no. 1 (2008): 66-79.
14. Le, Taoran, Vasileios Lakafosis, Sangkil Kim, Benjamin Cook, Manos M. Tentzeris, Ziyin Lin, and Ching-ping Wong. "A novel graphene-based inkjet-printed WISP-enabled wireless gas sensor." In *Microwave Conference (EuMC), 2012 42nd European*, pp. 412-415. IEEE, 2012.
15. Kim, Sangkil, Benjamin Cook, Taoran Le, James Cooper, Hoseon Lee, Vasileios Lakafosis, Rushi Vyas et al. "Inkjet-printed antennas, sensors and circuits on paper substrate." *IET Microwaves, Antennas & Propagation* 7, no. 10 (2013): 858-868.
16. [http://www.cabot-corp.com/ CCI-300 Data Sheet](http://www.cabot-corp.com/CCI-300>DataSheet).
17. Lin, Ziyin, Yagang Yao, Zhuo Li, Yan Liu, Zhou Li, and Ching-Ping Wong. "Solvent-assisted thermal reduction of graphite oxide." *The Journal of Physical Chemistry C* 114, no. 35 (2010): 14819-14825.
18. Li, Zhuo, Yagang Yao, Ziyin Lin, Kyoung-Sik Moon, Wei Lin, and Chingping Wong. "Ultrafast, dry microwave synthesis of graphene sheets." *Journal of Materials Chemistry* 20, no. 23 (2010): 4781-4783.
19. Hummers Jr, William S., and Richard E. Offeman. "Preparation of graphitic oxide." *Journal of the American Chemical Society* 80, no. 6 (1958): 1339-1339.
20. Leenaerts, O., B. Partoens, and F. M. Peeters. "Adsorption of H<sub>2</sub>O, N<sub>2</sub>, CO, N<sub>2</sub>O, and NO on graphene: A first-principles study." *Physical Review B* 77, no. 12 (2008): 125416.